THE ASTROPHYSICAL JOURNAL, Vol. 152, May 1968

OBSERVATIONS OF THE ANGULAR STRUCTURE OF RADIO SOURCES

F. N. BASH*

Leander McCormick Observatory, University of Virginia, Charlottesville, Virginia, and National Radio Astronomy Observatory,† Green Bank, West Virginia

Received July 26, 1967; revised October 30, 1967

ABSTRACT

Results of two-element interferometer observations of 234 radio sources are given. The interferometer operated at 2695 MHz with five antenna separations from 10000 to 24000λ. Source selection criteria, observing techniques, and reduction procedures are discussed. It is shown that apparently bright quasi-stellar sources have a higher mean fringe visibility than the apparently faint ones, while the apparently bright radio galaxies tend to have a lower mean fringe visibility than the apparently faint ones.

The quasi-stellar sources with flat radio spectra have a higher mean fringe visibility than those with steep spectra. No relation was found between mean fringe visibility and redshift for either the quasi-stellar sources or radio galaxies. At least 13 per cent and probably 62 per cent of the sources observed have at least two radiating components.

I. INTRODUCTION

This paper reports the results of observations of 234 radio sources using the two-element interferometer at the National Radio Astronomy Observatory. The sources were observed at five of the six possible element spacings in order to construct one-dimensional brightness distributions of the sources by model fitting. A subsequent paper will include models of the brightness distributions for the sources observed and analyses using angular sizes derived from the models.

Interferometric investigations of the brightness distributions of large numbers of radio sources have been made by several groups. Allen, Anderson, Conway, Palmer, Reddish, and Rowson (1962) have examined 384 radio sources at 158 MHz using antenna separations of 2200, 9700, 32000, and 61000λ. Their study suffered from an rms uncertainty in the fringe amplitude of 20–30 per cent, and the analysis (Allen, Brown, and Palmer 1962) was done by examining the data in bulk, rather than source-by-source. Maltby (1962) and Moffet (1962) examined approximately 190 radio sources at 960 MHz, using separations of 195, 289, 779, and 1557λ. The rms noise fluctuations were about 0.4–0.8 flux units in amplitude, with gain calibration uncertainties of about 10 per cent. They made models for the brightness distributions of a large fraction of the sources observed. Lequeux (1962) observed forty radio sources at a maximum separation of 6950λ east-west and 1820λ north-south at 1420 MHz. The minimum detectable fringe amplitude was 1.5 flux units. Fomalont (1966) has observed 532 radio sources at 1425 MHz at spacings ranging from 144 to 2626λ east-west. The rms noise of his system was 0.08 flux units in a 6-min observation, which was less than the rms noise due to confusing sources in his antenna beams. The phase stability of his system allowed Fomalont to find the brightness distributions on many of his sources by a Fourier series inversion of the measured fringe visibilities.

II. DESCRIPTION OF THE INSTRUMENT AND SOURCE SELECTION CRITERIA

The variable spacing interferometer at the NRAO consisted of two 85-foot-diameter antennas, operating at 2695 MHz. They could be spaced at six separations in 300-meter steps from 1.2 through 2.7 km, along a line oriented at azimuth 242°. The interferometer

* Present address: Astronomy Department, University of Texas.

† Operated by Associated Universities, Inc., under contract with the National Science Foundation.

operated on the double side-band principle with an intermediate-frequency band width of 10 MHz and center frequency of 7 MHz. In order to observe radio sources with fringes near zero order, time delays were inserted in the intermediate-frequency cables (see, e.g., Read 1962). A unit of delay was inserted every 32 fringes. Frequent checks were made on the time at which the delay was inserted, by observing the change in fringe amplitude for the calibration sources at the time of delay insertion. If the delay was inserted at the correct time, the fringe amplitude did not change. The system noise-temperature for the observations at the 2.1-km separation was about 290° K, while the remaining observations were taken with an improved receiving system with noise temperature about 130° K, resulting in rms output amplitude fluctuations of 1.8 and 0.83 flux units, respectively, in a 0.1-sec integration period. The sources in the program were observed at all but the 2.4-km separation. Clark and Hogg (1966) have observed 146 radio sources at this spacing.

The source list consists of three groups:

1. The 149 radio sources in the resurvey by Pauliny-Toth, Wade, and Heeschen (1966) of the 3C and 3CR catalogues, having 1400 MHz flux densities greater than 2×10^{-26} W m^{-2} Hz^{-1}, $|b^{\rm II}| > 20°$, and angular diameters less than about 4′ were selected. One of these sources, 3C 61.1, which is above the northern telescope limits, was excluded.

2. A list of 56 additional, mostly fainter, sources was included in June 1965. These were known or suspected to be quasi-stellar. At this writing the observing list contains 49 confirmed quasi-stellar sources, of which measured redshifts are available for 44. Twenty-eight of the 49 quasi-stellar sources appear in Group 1.

3. A final group of 19 radio sources was chosen from previous published work on brightness distributions. It was felt that long, base-line observations of these sources might be a valuable aid to understanding their structure.

III. OBSERVING AND DATA-REDUCTION PROCEDURES

Three 15-min observations were made on each source, at each of the five antenna separations used, as near as possible to its crossing of the instrumental equator. (The instrumental equator is the great circle defined by the intersection of the celestial sphere and the plane which is perpendicular to the base line.) Observing on the instrumental equator gives the highest resolution; however, the position angle of the direction of resolution is a function of declination. The right-ascension and declination components of the projection of the base line in wavelengths on a plane tangent to the celestial sphere at the source position are called u and v, respectively (see Rowson 1963). The position angle of the direction of resolution, σ, is given by

$$\tan \sigma = \frac{u}{v} ,$$

and the projected base-line length (in wavelengths) in the direction σ by

$$w = (u^2 + v^2)^{1/2} .$$

Sources at declinations exceeding $\delta = 65°$ do not cross the instrumental equator; these were observed at an hour angle of $-1^{\rm h}10^{\rm m}$, where the fringe frequency is maximum.

The positions for the 3C, 3CR, and NRAO sources were taken from the work of Pauliny-Toth *et al.* (1966). The Parkes source positions were taken from Day, Shimmins, Ekers, and Cole (1966). The MSH source positions were taken from Mills, Slee, and Hill (1958) and checked against a preprint of the southern Parkes survey (Shimmins, Day, Ekers, and Cole 1966).

The output of the NRAO interferometer was integrated for 0.1-sec periods and recorded on magnetic tape along with the indicated positions of the two antennas and other data. The data were analyzed with an IBM 7040 computer using a program written by B. G. Clark and C. M. Wade.

The program takes the 1950.0 position for each source, precesses it to the date and time of the observation, adjusts it for aberration and nutation, calculates the fringe frequency, and fits a sinusoid of this frequency (plus a constant term) to each minute of the data. The program calculates the amplitude and phase of the best-fitting sinusoid and the value of the constant using the least-squares principle. The program also furnishes the rms difference between the interferometer output and the fitted curve plus the difference between the precessed source position and the recorded indicated positions, allowing detection of interference and accidental mispointing of the antennas.

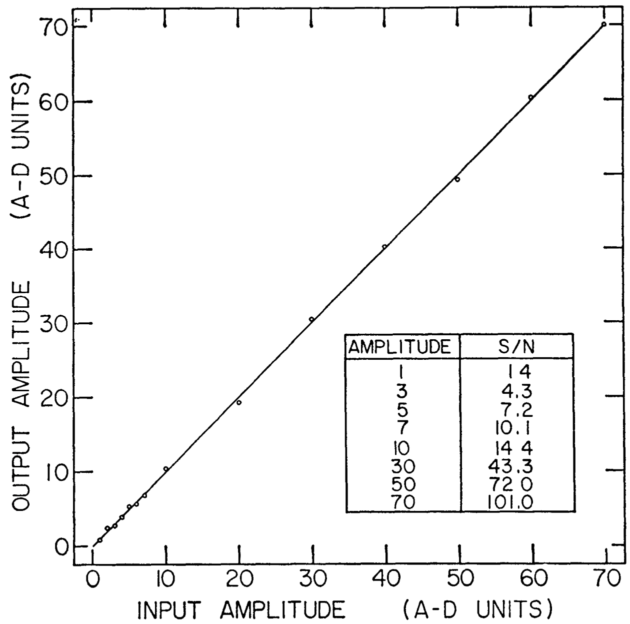

FIG. 1.—Results of the test of the reduction program. The fringe amplitude is in units of the least significant digit of the analogue-to-digital converter (*A–D* units).

The accuracy of this program was tested by having it reduce some "fringes" of known signal-to-noise ratio which were generated in the computer. The result of this test is shown in Figure 1. The line at 45° is drawn in. The test shows that the output of the reduction program is equal to the input fringe amplitude to within 2.5 per cent over the range of fringe amplitudes observed. The minimum fringe amplitude observed was equivalent to about 1 unit in Figure 1.

The gain of the interferometer was calibrated using the calibration sources listed in Table 1. They are all unresolved except for 3C 380, which is only slightly resolved. The fringe amplitude of 3C 380 as a function of hour angle was determined in a set of separate calibration observations. The fringe amplitude of 3C 380, measured at the celestial meridian, is listed in Table 1.

The apparent fringe amplitude of an unresolved source changed with hour angle. The interferometer was equipped with an automatic level control loop. At large zenith angles, when some of the antenna side lobes pointed toward the ground, the system noise-temperature rose. The automatic level control loop decreased the system gain so that both input levels to the correlator were constant. Most of the apparent change in fringe amplitude is thought to be due to this effect. The effect was calibrated by observing the unresolved calibration sources over a wide range of hour angle. The maximum correction within zenith angle 60° was 3 per cent. All sources except MSH 00−2,9 were observed within this zenith-angle range. At the zenith angle at which MSH 00−2,9 was observed ($Z = 73°$), the correction was 5 per cent.

The actual values of the fringe amplitudes of the calibration sources, in flux units, were determined by the following calibration process. The ratios of the fringe amplitudes of the calibration sources were first determined by a series of observations in which a given calibration source was observed for about 30 min, then another, etc., for 2 to 3 days. By least squares, the ratio of the fringe amplitude of each calibrator relative to 3C 286 was calculated. If the flux density of 3C 286 was very accurately known, the fringe amplitude of each source, in flux units, could be obtained by multiplying each ratio by the known flux density of 3C 286. Instead of this latter process, we felt that the average of the flux densities of the calibration sources was a more accurately known quantity. Thus, the sum of the fringe-amplitude ratios was divided into the sum of the flux densities of the calibration sources measured by Kellermann (private communication). The quotient is the flux density of 3C 286 on the interferometer's flux-density system. We then multiplied each ratio of the fringe amplitudes of the other calibrators relative to 3C 286 by this flux density to obtain the flux density of each other calibration source. 3C 380 was not included in the ratio or flux-density sums mentioned above, since it was partially resolved.

TABLE 1

FLUX DENSITIES OF THE CALIBRATION SOURCES AT THE FIVE ANTENNA SEPARATIONS IN THE ORDER IN WHICH THEY WERE OBSERVED

Calibration Source	2 1 Km*	2 7 Km	1 2 Km	1 8 Km	1 5 Km
3C 48 ...	8 61†	8 38	8 37	8 44	8 45
3C 147 ..	12 34	12 39	12 35	12 59	12 63
3C 286....	9 41	10 03	10 03	10 08	10 14
3C 345	6 43	5 92	5 99	5 68	5 57
3C 380 (meridian)	7 75	7 39	8 74	8 54	8 71
CTA 102	4 70	5 08	5 06	5 02	5 02
Dates of observations.......	7/16/65–8/5/65	11/8/65–11/25/65	1/6/66–1/18/66	2/14/66–3/8/66	4/16/66–5/3/66

* The antenna feed horns were aligned with their E-vectors in position-angle 90° The remainder are in position-angle 0°.

† In units of 10^{-26} W m^{-2} Hz^{-1} at 2695 MHz.

The flux densities of the calibration sources obtained by this process appear in Table 1 in the order in which the interferometer stations were occupied. The flux density quoted for 3C 380 is the fringe amplitude measured at the celestial meridian. It can be seen that the flux density of 3C 345 varied with time, as has been found by Dent (1965) at 8000 MHz and by Bartlett (1966) at 2700 MHz; the remainder are constant to ± 2 per cent for the antenna separations other than 2.1 km. The flux densities at 2.1 km differ because the feed horns were inadvertently rotated 90°, and some of the calibration sources are polarized.

3C 345 was used as a calibration source even though it varied because three independent measures of its flux density were made by Kellermann during the course of these observations; thus the time variation was known and taken into consideration in the calibration process mentioned above. 3C 380 was used as a secondary calibration source. It was observed daily at the same hour angle in order to determine variations in the system gain. As is mentioned above, it was not included in the flux-density calibration calculations since it was resolved.

During the course of the observations reported here, a calibration source was observed about every 4 hours, always within 2 hours of the meridian. The interference fringes were recorded using an analogue-to-digital converter and were in units of the least significant digit of that converter, called "*A–D* units."

The observed fringe amplitude for the calibration sources and their derived flux densities were used to calculate the system gain as a function of time in terms of *A–D* units/flux unit. All observations were calibrated using this curve.

The curve of system gain as a function of time varied during the course of a day by about 3–4 per cent of its mean value. The rms scatter in the fringe-amplitude measurements of a given source, each separated by 4 days, and calibrated with the system-gain curve was typically 3 per cent or 0.03 flux units, whichever is greater.

The system phase has been observed to drift slowly by amounts of 1°/min up to occasionally 3°–4°/min. This has two effects. First, in order to calculate a vector average fringe amplitude and phase for each 15-min observation, the fringe phase, determined each minute, must be used. If the instrumental phase is drifting, the vector average amplitude must be corrected. It can be easily shown that this correction factor is $(\Delta\Phi/2)/(\sin \Delta\Phi/2)$, where $\Delta\Phi$ is the drift in phase in radians during the 15-min observation. Second, the drifting phase causes one to need to frequently calibrate the system phase, so that the three observations of a given source, each separated by 4 days, may be corrected to the same system phase. This latter calibration process was not done, since too much time was required, and the number of sources observed would have been decreased. Thus we have measured the fringe amplitudes only.

A phase drift of 100° during one 15-min observation was adopted as the maximum allowed (maximum correction factor of 1.11). If the phase drift exceeded 100° the observation was rejected. This has undoubtedly caused the rejection of a few perfectly good observations in which the phase drift was a result of source structure; however, we felt that system malfunctions or source position errors were the more likely cause of large phase drifts. (A source position error of 0′.6 can cause a drift of 100° in 15 min in the worst case.)

IV. RESULTS OF THE OBSERVATIONS

The average fringe amplitude from three 15-min measurements of the fringe amplitude for each source at each of five base lines is given in Table 2. If the average fringe amplitude was less than twice its rms error, it was arbitrarily set to zero, giving a fringe visibility of zero. The antenna feed horns were aligned with their *E*-vectors in position-angle 0°, except for the observations at the 2.1-km spacing where they were inadvertently aligned at position-angle 90°.

The columns in Table 2 are, in order: the source name; the 2695 MHz total flux density measured by Kellermann, Pauliny-Toth, and Tyler (1967); the estimated probable error of flux density; the fringe visibility; the visibility probable error; the base-line length, in wavelengths, in the direction of resolution for the five antenna separations; the position angle of the direction of resolution for each source; and finally the class of the object. The flux densities furnished by Kellermann *et al.* in Table 2 are preliminary values. The numbers 1, 2, and 3 refer to the source groups previously defined in § II, while *G* and *Q* indicate identified radio galaxies and quasi-stellar sources, respectively, taken from the lists of Wyndham (1966); Burbidge, Burbidge, Hoyle, and Lynds (1966); Schmidt (1966*a*, *b*); Ford and Rubin (1966); Lynds, Stockton, and Livingston (1965); and Lynds, Hill, Heere, and Stockton (1966). The sources are marked "*P*" when all measured fringe visibilities exceed 0.8.

In the case of MSH 05−1,3, no flux density measurement was available. Therefore, the fringe amplitude, in flux units, is given instead of the fringe visibility.

The flux density of "confusing sources" in the antenna beams has been calculated using the 3CR survey (Bennett 1962) and the CTD survey (Kellermann and Read 1965). These calculations give 0.05 and 0.04 flux units for the two surveys, respectively. Since the background of confusing sources is not likely to consist of entirely unresolved sources, on the average, the fringe amplitude caused by the confusing sources would be

3C 120.0 4.9 0.04 0.54 0.03 10786. 0.56 0.03 13482. 0.47 0.03 16179. 0.50 0.03 18876. 0.55 0.03 24269. 67.77 1

TABLE 2

THE MEASURED FRINGE VISIBILITIES

(The flux density [($S2695$)] and its probable error [p.e.] are expressed in flux units [10^{-26} W m^{-2} Hz^{-1}]. The fringe visibility and its probable error are expressed in visibility units. The antenna separation projected in the direction of the source (w) is expressed in wavelengths. The position angle of the direction of resolution (P.A.) is expressed in degrees.)

SOURCE	S(2695MHZ)	P.E.	1.2KM VIS.	1.2KM P.E.	1.2KM W	1.5KM VIS.	1.5KM P.E.	1.5KM W	1.8KM VIS.	1.8KM P.E.	1.8KM W	2.1KM VIS.	2.1KM P.E.	2.1KM W	2.7KM VIS.	2.7KM P.E.	2.7KM W	P.A.	CLASS
3C 2.0	2.2	0.04	0.87	0.03	10787.	0.84	0.03	13455.	0.78	0.06	16179.	0.75	0.04	18871.	0.65	0.03	24270.	67.88	2,Q
3C 5.0	0.9	0.04	0.47	0.03	10787.	0.34	0.03	13476.	0.49	0.03	16180.	0.38	0.06	18876.	0.43	0.03	24269.	67.88	3
3C 9.0	1.0	0.04	0.97	0.03	10786.	0.85	0.03	13482.	0.84	0.03	16179.	0.58	0.05	18876.	0.62	0.03	24270.	66.97	2,Q
MSH00-2,9	1.5	0.04	0.19	0.03	10780.	0.11	0.03	13476.	0.08	0.03	16172.	0.07	0.03	18867.				65.45	2
3C 13.0	0.9	0.04	0.85	0.03	10783.	0.85	0.04	13478.	0.80	0.03	16175.	0.74	0.05	18870.	0.66	0.03	24260.	59.49	3
3C 15.0	2.3	0.04	0.56	0.03	10787.	0.44	0.03	13479.	0.35	0.03	16180.	0.23	0.03	18876.	0.20	0.03	24269.	67.89	1,G
3C 17.0	3.7	0.04	0.37	0.03	10787.	0.28	0.03	13482.	0.23	0.03	16179.	0.21	0.03	18876.	0.23	0.03	24270.	67.88	1,G
3C 18.0	2.6	0.04	0.34	0.03	10786.	0.21	0.03	13481.	0.11	0.03	16179.	0.0	0.03	18874.	0.04	0.03	24267.	67.41	1,G
3C 19.0	1.9	0.04	0.73	0.03	10787.	0.61	0.03	13482.	0.47	0.03	16179.	0.32	0.03	18876.	0.13	0.03	24269.	63.24	1
3C 29.0	3.3	0.05	0.09	0.03	10787.	0.08	0.03	13481.	0.06	0.03	16180.	0.04	0.03	18876.	0.03	0.03	24269.	67.89	1,G
3C 32.0	2.0	0.04	0.12	0.03	10786.	0.37	0.03	13482.	0.15	0.03	16180.	0.22	0.03	18876.	0.0	0.03	24270.	66.96	1
3C 33.0	7.5	0.07	0.36	0.03	10787.	0.39	0.03	13482.	0.32	0.03	16180.	0.17	0.03	18876.	0.22	0.03	24269.	67.22	1,G
3C 36.0	0.6	0.04	0.51	0.04	10776.	0.32	0.04	13468.	0.09	0.04	16164.	0.17	0.08	18856.	0.48	0.04	24244.	54.36	2
3C 38.0	2.6	0.04	0.40	0.03	10786.	0.36	0.03	13482.	0.42	0.03	16179.	0.59	0.05	18876.	0.62	0.03	24270.	67.07	1
3C 39.0	0.5	0.04	0.26	0.05	10786.	0.29	0.05	13482.	0.08	0.05	16180.	0.0	0.05	18876.	0.19	0.05	24269.	67.83	2
3C 41.0	2.2	0.04	0.91	0.03	10787.	0.87	0.04	13481.	0.81	0.04	16179.	0.65	0.03	18876.	0.63	0.03	24269.	63.14	1
3C 42.0	1.6	0.05	0.11	0.03	10786.	0.38	0.03	13482.	0.63	0.03	16179.	0.75	0.04	18875.	0.58	0.03	24268.	64.23	1
3C 43.0	1.7	0.05	0.98	0.03	10787.	0.97	0.04	13482.	0.96	0.07	16180.	0.98	0.04	18876.	0.98	0.04	24269.	65.73	2,Q,P
3C 44.0	0.7	0.05	0.53	0.04	10787.	0.35	0.04	13482.	0.54	0.04	16180.	0.38	0.06	18876.	0.34	0.04	24269.	67.73	2
3C 46.0	0.6	0.04	0.16	0.04	10774.	0.13	0.04	13466.	0.12	0.04	16160.	0.0	0.07	18852.	0.0	0.04	24237.	58.98	2,G
3C 45.0	1.3	0.05	0.73	0.03	10786.	0.65	0.03	13481.	0.52	0.03	16179.	0.52	0.05	18876.	0.29	0.03	24270.	67.62	1
3C 47.0	2.0	0.04	0.38	0.03	10783.	0.30	0.03	13479.	0.15	0.03	16176.	0.27	0.03	18871.	0.33	0.03	24260.	65.67	2,Q
3C 48.0	8.9	0.06	CALIBRATOR																,Q,P
3C 49.0	1.5	0.04	0.96	0.03	10786.	0.92	0.03	13482.	0.95	0.04	16180.	0.94	0.04	18876.	0.96	0.03	24269.	67.14	1,P
3C 54.0	1.0	0.06	0.58	0.03	10784.	0.60	0.05	13478.	0.31	0.03	16175.	0.62	0.06	18871.	0.53	0.04	24262.	57.19	3
3C 55.0	1.3	0.05	0.55	0.03	10751.	0.28	0.03	13439.	0.0	0.03	16129.	0.36	0.03	18814.	0.31	0.03	24178.	61.62	2
3C 57.0	1.9	0.06	0.95	0.03	10786.	0.92	0.05	13481.	0.95	0.04	16178.	0.94	0.06	18875.	0.96	0.04	24267.	67.55	1,P
NRAO 91	3.0	0.04	0.94	0.03	10783.	0.93	0.03	13478.	0.90	0.06	16175.	0.97	0.04	18871.	0.96	0.04	24259.	66.63	1,P
3C 59.0	1.3	0.09	0.17	0.03	10769.	0.15	0.03	13460.	0.04	0.03	16153.	0.16	0.04	18843.	0.11	0.03	24225.	62.25	1
3C 62.0	2.7	0.04	0.24	0.03	10783.	0.21	0.03	13477.	0.14	0.03	16173.	0.20	0.03	18869.	0.14	0.03	24258.	67.67	1
3C 63.0	1.6	0.04	0.25	0.03	10787.	0.41	0.03	13481.	0.37	0.03	16180.	0.24	0.03	18876.	0.10	0.03	24270.	67.89	1,G
3C 64.0	1.4	0.05	0.20	0.03	10787.	0.24	0.03	13481.	0.30	0.03	16180.	0.13	0.03	18875.	0.23	0.03	24269.	67.60	1
3C 67.0	1.7	0.04	0.99	0.03	10767.	0.98	0.03	13459.	1.00	0.03	16154.	0.98	0.03	18844.	0.95	0.03	24218.	62.79	1,G,P
3C 68.1	1.4	0.04	0.89	0.03	10738.	0.83	0.03	13423.	0.79	0.03	16107.	0.78	0.03	18794.	0.65	0.03	24153.	58.50	1
3C 71.0	3.0	0.04	0.45	0.03	10767.	0.37	0.03	13452.	0.32	0.03	16145.	0.30	0.03	18835.	0.26	0.03	24206.	67.85	1,G
3C 75.0	3.4	0.06	0.03	0.03	10763.	0.01	0.03	13455.	0.02	0.03	16148.	0.03	0.03	18839.	0.02	0.03	24215.	67.30	1,G
3C 76.0	0.4	0.05	1.07	0.07	10787.	1.01	0.07	13482.	0.97	0.07	16180.	0.87	0.13	18876.	0.78	0.07	24270.	53.42	3
3C 76.1	1.9	0.04	0.0	0.15	10760.	0.0	0.14	13450.	0.0	0.13	16141.	0.0	0.17	18831.	0.0	0.12	24203.	65.55	1,G
3C 78.0	5.0	0.09	0.17	0.03	10764.	0.18	0.03	13453.	0.18	0.03	16146.	0.19	0.03	18836.	0.17	0.03	24223.	67.50	1,G
3C 79.0	2.4	0.04	0.20	0.03	10724.	0.27	0.03	13404.	0.19	0.03	16083.	0.22	0.03	18767.				64.59	1,G
3C 86.0	4.5	0.15	0.60	0.03	10787.	0.42	0.04	13482.				0.32	0.03	18876.	0.16	0.03	24270.	48.48	3
3C 88.0	2.8	0.04	0.03	0.03	10748.	0.05	0.03	13434.	0.05	0.03	16121.	0.05	0.03	18807.	0.04	0.03	24176.	67.56	1,G
3C 89.0	1.3	0.04	0.22	0.03	10717.	0.18	0.03	13402.	0.13	0.03	16086.	0.0	0.03	18768.	0.07	0.03	24124.	67.90	1,G
3C 93.0	1.5	0.04	0.25	0.03	10724.	0.23	0.03	13410.	0.18	0.03	16093.	0.24	0.03	18777.	0.13	0.03	24133.	67.13	2,Q
3C 95.0	1.4	0.04	0.39	0.03	10770.	0.38	0.03	13463.	0.28	0.03	16158.	0.16	0.03	18842.	0.11	0.03	24231.	67.96	1,Q
MSH03-1,9	1.4	0.50	0.37	0.03	10749.	0.36	0.03	13439.	0.30	0.03	16127.	0.19	0.04	18815.	0.07	0.03	24174.	68.37	2,Q
3C 94.0	1.3	0.05	0.86	0.03	10709.	0.65	0.04	13384.	0.75	0.04	16063.	0.52	0.03	18740.	0.59	0.03	24090.	68.48	1
3C 98.0	6.5	0.40	0.03	0.03	10773.	0.02	0.03	13465.	0.0	0.05	16159.	0.02	0.03	18851.	0.01	0.03	24237.	66.90	1,G
3C 105.0	3.3	0.05	0.49	0.03	10775.	0.48	0.03	13468.	0.49	0.03	16163.	0.47	0.03	18856.	0.41	0.03	24241.	67.64	1
3C 107.0	0.7	0.04	0.37	0.04	10769.	0.26	0.04	13462.	0.28	0.04	16156.	0.38	0.06	18847.	0.46	0.04	24225.	67.92	2
3C 109.0	2.4	0.05	0.55	0.03	10785.	0.41	0.03	13481.	0.10	0.03	16179.	0.21	0.03	18874.	0.10	0.03	24267.	67.28	1,G
3C 111.0	9.5	0.10	0.11	0.03	10787.	0.22	0.03	13482.	0.05	0.03	16180.	0.26	0.03	18876.	0.17	0.03	24270.	61.37	3
3C 119.0	5.3	0.04	0.95	0.03	10787.	0.97	0.03	13482.	0.96	0.03	16180.	0.95	0.04	18876.	0.97	0.03	24270.	59.65	2,Q,P

TABLE 2—*Continued*

SOURCE	S(2695MHZ)	P.E.	1.2KM VIS.	1.2KM P.E.	1.2KM W	1.5KM VIS.	1.5KM P.E.	1.5KM W	1.8KM VIS.	1.8KM P.E.	1.8KM W	2.1KM VIS.	2.1KM P.E.	2.1KM W	2.7KM VIS.	2.7KM P.E.	2.7KM W	P.A.	CLASS
NRAO 190	4.2	0.04	0.87	0.03	10785.	0.86	0.04	13479.	0.89	0.05	16177.	0.88	0.07	18872.	0.87	0.04	24264.	67.89	1,P
3C 134.0	4.2	0.04	0.06	0.03	10786.	0.06	0.03	13482.	0.03	0.03	16180.	0.02	0.03	18876.	0.02	0.03	24270.	61.30	3
MSH05-1,3			0.08	0.03	10786.	0.06	0.03	13481.	0.04	0.03	16179.	0.09	0.03	18875.	0.06	0.03	24268.	66.82	2
3C 135.0	1.7	0.04	0.43	0.03	10787.	0.15	0.03	13481.	0.33	0.03	16179.	0.14	0.03	18876.	0.22	0.03	24211.	67.86	1,G
3C 138.0	5.9	0.04	1.01	0.03	10787.	1.03	0.03	13482.	1.00	0.06	16180.	0.81	0.03	18875.	0.98	0.03	24269.	66.82	2,Q,P
3C 147.0	12.9	0.04	CALIBRATOR																,Q,P
3C 152.0	0.8	0.04	0.80	0.03	10786.	0.79	0.03	13482.	0.73	0.03	16180.	0.73	0.06	18876.				56.24	2
3C 153.0	2.3	0.04	0.57	0.03	10778.	0.41	0.03	13471.	0.23	0.03	16167.	0.21	0.03	18860.	0.41	0.03	24247.	52.42	3,G
3C 154.0	3.1	0.04	0.62	0.03	10786.	0.67	0.03	13482.	0.62	0.03	16180.	0.24	0.03	18876.	0.43	0.03	24269.	65.13	2
3C 158.0	1.1	0.04	0.93	0.03	10787.	0.86	0.03	13482.	0.86	0.06	16180.	0.77	0.07	18876.	0.67	0.03	24269.	67.06	2
3C 159.0	1.1	0.05	0.41	0.03	10776.	0.39	0.03	13468.	0.74	0.03	16164.	0.29	0.04	18858.	0.59	0.03	24245.	57.98	2
3C 161.0	10.7	0.04	0.79	0.03	10787.	0.80	0.03	13482.	0.79	0.04	16180.	0.60	0.03	18875.	0.82	0.03	24269.	67.79	2
3C 165.0	1.3	0.05	0.22	0.03	10787.	0.15	0.03	13482.	0.14	0.04	16180.	0.16	0.04	18876.	0.0	0.03	24270.	65.73	2
3C 171.0	2.0	0.04	0.38	0.03	10787.	0.23	0.03	13482.	0.12	0.03	16180.	0.08	0.03	18876.	0.21	0.03	24269.	49.82	1,G
3C 173.0	0.9	0.04	0.88	0.03	10787.	0.90	0.04	13482.	0.84	0.03	16180.	0.81	0.07	18876.	0.74	0.05	24269.	51.35	2
3C 173.1	1.4	0.04	0.53	0.03	10047.	0.25	0.03	12577.	0.16	0.03	15076.	0.29	0.03	17598.	0.0	0.06	22625.	83.69	1,G
3C 178.0	0.5	0.15	0.51	0.07	10787.	0.82	0.10	13481.	0.89	0.10	16179.	0.66	0.12	18876.	0.42	0.05	24269.	67.61	2
3C 179.0	1.5	0.07	0.11	0.03	10110.	0.23	0.03	12640.	0.36	0.03	15170.	0.22	0.05	17706.	0.43	0.03	22763.	81.14	1
3C 181.0	1.2	0.04	0.76	0.03	10778.	0.68	0.03	13470.	0.58	0.03	16167.	0.45	0.07	18859.	0.21	0.03	24243.	66.38	2,Q
3C 184.0	1.2	0.04	0.87	0.05	10182.	0.80	0.04	12729.	0.70	0.05	15273.	0.44	0.05	17822.	0.27	0.03	22926.	77.97	1
3C 184.1	1.7	0.10	0.21	0.03	10067.	0.18	0.03	12581.	0.0	0.06	15100.	0.19	0.04	17620.	0.13	0.03	22658.	81.69	1,G
3C 186.0	0.6	0.10	0.73	0.05	10787.	0.75	0.04	13482.	0.74	0.06	16180.	0.73	0.10	18876.	0.83	0.10	24270.	61.32	2,Q
NRAO 276	1.8	0.04	0.13	0.03	10785.	0.14	0.03	13480.	0.14	0.03	16177.	0.14	0.03	18874.	0.11	0.03	24256.	50.71	1
3C 190.0	1.3	0.06	0.98	0.03	10787.	0.98	0.03	13482.	0.94	0.04	16180.	0.89	0.07	18876.	0.76	0.03	24269.	67.09	1
3C 191.0	0.9	0.04	0.84	0.03	10787.	0.95	0.04	13482.	0.91	0.06	16180.	0.93	0.04	18876.	0.87	0.03	24270.	67.46	2,Q,P
3C 192.0	3.1	0.04	0.06	0.03	10787.	0.07	0.03	13482.	0.07	0.03	16180.	0.09	0.03	18876.	0.06	0.03	24269.	65.52	1,G
3C 194.0	1.1	0.20	0.87	0.04	10782.	0.82	0.03	13476.	0.78	0.06	16173.	0.72	0.06	18868.	0.51	0.04	24258.	57.37	1
3C 196.0	7.6	0.04	0.64	0.03	10781.	0.50	0.03	13474.	0.32	0.03	16170.	0.17	0.03	18864.	0.25	0.03	24254.	52.77	2,Q
3C 198.0	1.0	0.04	0.0	0.03	10787.	0.0	0.03	13481.	0.0	0.03	16180.	0.0	0.03	18875.	0.0	0.03	24269.	67.74	1,G
3C 204.0	0.5	0.04	0.0	0.05	10140.	0.79	0.06	12677.	0.56	0.08	15212.	0.21	0.08	17750.	0.29	0.06	22803.	80.24	2,Q
3C 205.0	1.0	0.01	0.60	0.03	10784.	0.84	0.04	13478.	0.83	0.03	16175.	0.74	0.06	18871.	0.54	0.03	24258.	41.16	1
3C 207.0	1.7	0.07	0.53	0.03	10786.	0.38	0.03	13482.	0.16	0.03	16179.	0.08	0.03	18875.	0.13	0.03	24270.	67.19	1,Q
3C 208.0	0.9	0.04	0.57	0.03	10787.	0.77	0.03	13482.	0.90	0.03	16180.	0.94	0.08	18876.	0.68	0.03	24269.	67.09	2,Q
3C 208.1	1.2	0.05	0.81	0.04	10786.	0.77	0.03	13480.	0.70	0.03	16178.	0.59	0.05	18874.	0.55	0.03	24267.	66.94	1
3C 210.0	0.9	0.10	0.77	0.07	10785.	0.72	0.03	13480.	0.65	0.04	16177.	0.59	0.08	18872.				64.10	3
3C 212.0	1.4	0.10	0.93	0.03	10781.	0.85	0.03	13476.	0.62	0.03	16173.	0.64	0.08	18868.	0.63	0.03	24257.	66.63	1,G
3C 215.0	0.7	0.08	0.13	0.04	10784.	0.14	0.04	13480.	0.20	0.04	16177.	0.21	0.07	18873.	0.0	0.05	24265.	66.47	2,Q
3C 217.0	1.0	0.04	0.28	0.03	10767.	0.0	0.03	13460.	0.32	0.04	16153.	0.54	0.09	18844.	0.76	0.07	24228.	58.39	2
3C 216.0	2.4	0.07	0.92	0.03	10783.	0.92	0.04	13478.	0.87	0.03	16174.	0.84	0.04	18870.	0.77	0.04	24260.	57.31	2,Q
3C 218.0	22.4	0.20	0.16	0.03	10787.	0.20	0.03	13482.	0.15	0.03	16180.	0.11	0.03	18876.	0.10	0.03	24269.	67.43	1,G
3C 219.0	4.3	0.05	0.09	0.03	10785.	0.03	0.03	13480.	0.01	0.03	16177.	0.02	0.03	18873.	0.04	0.03	24266.	56.16	1,G
3C 220.1	1.0	0.05	0.52	0.03	10035.	0.0	0.03	12548.	0.39	0.05	15058.	0.22	0.06	17567.				84.41	1
3C 220.2	1.0	0.05	0.36	0.03	10780.	0.14	0.03	13472.	0.30	0.03	16168.	0.46	0.07	18862.	0.83	0.03	24250.	60.33	2
3C 220.3	1.3	0.08	0.57	0.03	10003.	0.43	0.03	12510.	0.30	0.04	15008.	0.23	0.03	17511.	0.30	0.05	22525.	87.05	1,G
3C 223.0	1.9	0.04	0.07	0.03	10779.	0.04	0.03	13473.	0.03	0.03	16170.	0.0	0.03	18864.	0.0	0.05	24253.	60.51	1,G
3C 225.0	2.0	0.06	0.87	0.03	10757.	0.50	0.06	13448.	0.60	0.07	16139.	0.72	0.06	18828.				65.99	2
3C 226.0	1.2	0.04	0.38	0.03	10778.	0.14	0.03	13471.				0.27	0.05	18860.	0.58	0.03	24248.	67.07	1,G
3C 227.0	4.1	0.05	0.15	0.03	10783.	0.07	0.03	13478.	0.10	0.03	16175.	0.09	0.03	18871.	0.02	0.03	24262.	67.48	1,G
3C 228.0	2.2	0.15	0.48	0.03	10770.	0.11	0.03	13461.	0.42	0.03	16154.	0.38	0.04	18846.	0.34	0.03	24231.	66.18	2
3C 230.0	1.3	0.20	1.05	0.03	10787.	1.05	0.06	13482.	0.97	0.06	16179.	1.07	0.08	18876.	0.94	0.05	24269.	67.89	2,P
3C 231.0	5.4	0.05	0.14	0.03	10105.	0.11	0.03	12637.	0.08	0.03	15167.	0.10	0.03	17691.	0.10	0.03	22760.	81.24	1,G
P0957+00	0.5	0.04	0.40	0.06	10777.	0.36	0.06	13469.	0.61	0.06	16164.	0.0	0.06	18858.	0.60	0.06	24246.	67.86	2,Q
3C 234.0	2.9	0.05	0.18	0.03	10779.	0.32	0.03	13472.	0.12	0.03	16168.	0.29	0.04	18862.	0.22	0.03	24250.	53.14	1,G
3C 235.0	0.3	0.05	0.78	0.08	10787.	0.70	0.08	13482.	0.67	0.08	16180.	0.64	0.16	18876.	0.39	0.08	24269.	55.25	3
3C 237.0	3.6	0.05	0.95	0.03	10780.	0.93	0.03	13473.	0.93	0.06	16169.	0.52	0.03	18863.	0.85	0.03	24253.	67.36	2

TABLE 2—*Continued*

SOURCE	S(2695MHZ)	P.E.	1.2KM VIS.	1.2KM P.E.	1.2KM W	1.5KM VIS.	1.5KM P.E.	1.5KM W	1.8KM VIS.	1.8KM P.E.	1.8KM W	2.1KM VIS.	2.1KM P.E.	2.1KM W	2.7KM VIS.	2.7KM P.E.	2.7KM W	P.A.	CLASS
3C 238.0	1.3	0.04	0.95	0.03	10775.	0.96	0.03	13466.	0.96	0.05	16159.	0.98	0.07	18852.	0.88	0.03	24237.	67.35	2,P
3C 241.0	0.7	0.04	0.99	0.04	10779.	0.97	0.04	13473.	0.96	0.07	16169.	0.94	0.11	18863.	0.95	0.04	24252.	65.06	2,P
3C 244.1	1.9	0.05				0.61	0.03	13480.	0.35	0.03	16179.	0.37	0.04	18874.				42.02	1,G
3C 245.0	2.1	0.04	0.82	0.03	10756.	0.76	0.03	13442.	0.69	0.05	16132.	0.53	0.06	18820.	0.50	0.03	24193.	66.23	2,Q
3C 246.0	1.2	0.05	0.09	0.03	10778.	0.48	0.03	13471.	0.55	0.03	16167.	0.13	0.03	18860.	0.32	0.03	24248.	67.98	1
3C 247.0	1.6	0.04	0.44	0.03	10786.	0.68	0.04	13482.	0.82	0.04	16180.	0.69	0.07	18876.	0.30	0.03	24269.	58.71	1
3C 249.0	1.3	0.04	0.42	0.03	10756.	0.23	0.03	13447.	0.27	0.03	16138.	0.45	0.05	18829.	0.78	0.03	24204.	67.91	1
3C 249.1	1.4	0.05	0.49	0.03	10111.	0.44	0.04	12640.	0.27	0.03	15165.	0.29	0.03	17697.	0.13	0.03	22757.	79.78	1,Q
3C 254.0	1.4	0.05	0.30	0.03	10782.	0.27	0.03	13475.	0.45	0.03	16172.	0.67	0.05	18867.	0.77	0.03	24256.	58.35	2,Q
3C 255.0	0.5	0.04	0.98	0.05	10772.	0.98	0.05	13463.	0.97	0.07	16158.	1.04	0.13	18850.	0.99	0.05	24235.	67.99	2,P
3C 256.0	0.6	0.04	1.00	0.05	10787.	0.98	0.05	13482.	0.98	0.05	16180.	0.96	0.10	18876.	0.97	0.05	24270.	65.64	2,G,P
3C 263.0	1.7	0.04	0.76	0.03	10136.	0.59	0.03	12672.	0.78	0.03	15205.	0.59	0.06	17740.	0.57	0.03	22855.	80.20	1,Q
NRAO 382	1.5	0.04	0.76	0.03	10786.	0.64	0.03	13482.	0.53	0.04	16180.	0.41	0.03	18876.	0.35	0.03	24269.	67.88	1
3C 263.1	1.5	0.04	0.56	0.03	10787.	0.36	0.03	13482.	0.17	0.03	16180.	0.09	0.03	18876.	0.43	0.03	24270.	65.92	1,G
3C 264.0	3.2	0.20	0.11	0.03	10787.	0.12	0.03	13482.	0.13	0.03	16179.	0.11	0.03	18875.	0.09	0.03	24269.	66.33	1,G
3C 265.0	1.4	0.04	0.26	0.03	10783.	0.48	0.03	13477.	0.46	0.03	16174.	0.29	0.04	18869.	0.30	0.03	24259.	62.63	1
3C 266.0	0.6	0.04	0.95	0.05	10783.	0.96	0.05	13477.	0.91	0.05	16174.	0.87	0.08	18870.	0.69	0.05	24260.	51.92	2
3C 267.0	1.3	0.04	0.82	0.03	10786.	0.47	0.03	13482.	0.74	0.03	16180.	0.49	0.04	18876.	0.55	0.03	24269.	67.22	1
NRAO 389	1.8	0.09	0.88	0.03	10779.	0.90	0.03	13472.	0.89	0.03	16169.	0.88	0.08	18863.	0.86	0.03	24250.	62.24	1,P
3C 268.1	3.9	0.10	0.85	0.03	10065.	0.68	0.03	12592.	0.82	0.03	15105.	0.72	0.06	17627.	0.67	0.03	22675.	82.83	1
3C 268.2	0.7	0.06	0.22	0.04	10781.	0.17	0.04	13474.	0.13	0.04	16171.	0.14	0.06	18865.	0.16	0.04	24254.	62.36	2,G
3C 268.3	2.0	0.05	0.97	0.03	10787.	0.99	0.03	13482.	0.96	0.03	16180.	0.92	0.07	18875.	0.96	0.03	24269.	27.91	1,P
3C 268.4	1.1	0.05	0.60	0.03	10784.	0.62	0.03	13479.	0.72	0.03	16176.	0.82	0.06	18871.	0.83	0.03	24262.	57.00	1,Q
3C 270.1	1.5	0.04	0.84	0.03	10780.	0.85	0.03	13474.	0.83	0.05	16170.	1.00	0.06	18867.	0.68	0.07	24255.	61.52	1,Q
3C 272.1	3.9	0.12	0.03	0.03	10780.	0.02	0.03	13473.	0.02	0.03	16170.	0.02	0.03	18864.	0.01	0.03	24252.	66.73	1,G
3C 273.0	40.7	0.40	0.88	0.03	10787.	0.77	0.03	13482.	0.57	0.03	16178.	0.68	0.05	18876.	0.75	0.03	24269.	67.86	2,Q
3C 274.1	1.4	0.04	0.14	0.03	10785.	0.14	0.03	13480.	0.11	0.03	16177.				0.06	0.03	24266.	65.70	1
3C 275.0	1.8	0.04	0.73	0.03	10782.	0.65	0.03	13478.	0.53	0.04	16175.	0.46	0.04	18870.	0.38	0.03	24260.	67.94	1
3C 275.1	1.5	0.07	0.86	0.03	10787.	0.81	0.03	13481.	0.73	0.05	16180.	0.69	0.05	18876.	0.58	0.03	24269.	56.75	2,Q
3C 277.1	1.4	0.07	0.89	0.04	10786.	0.90	0.05	13480.	0.88	0.07	16178.	0.88	0.09	18874.	0.89	0.09	24266.	44.70	2,Q,P
3C 277.3	1.9	0.05	0.11	0.03	10770.	0.04	0.03	13462.	0.07	0.03	16154.	0.07	0.03	18846.	0.09	0.03	24229.	62.87	1,G
3C 278.0	4.2	0.04	0.02	0.03	10784.	0.02	0.03	13480.	0.02	0.03	16178.	0.0	0.03	18874.	0.03	0.03	24266.	67.56	1,G
P1252+11	1.0	0.06	1.07	0.03	10780.	1.12	0.03	13473.	1.12	0.04	16168.	0.95	0.12	18863.	1.03	0.03	24251.	66.88	2,Q,P
3C 279.0	11.7	0.10	0.91	0.03	10773.	0.85	0.03	13467.	0.85	0.03	16160.	0.96	0.06	18854.	0.82	0.03	24241.	68.04	2,Q,P
3C 280.0	2.8	0.05	0.53	0.03	10778.	0.65	0.03	13472.	0.80	0.04	16167.	0.90	0.06	18862.	0.81	0.06	24249.	53.04	1
3C 280.1	0.6	0.04	0.32	0.05	10786.	0.66	0.05	13481.	0.82	0.07	16180.	0.83	0.08	18876.	0.44	0.05	24268.	60.18	2,Q
3C 281.0	0.5	0.10	0.53	0.05	10773.	0.30	0.05	13465.	0.45	0.05	16159.	0.0	0.10	18853.	0.50	0.05	24237.	67.31	2
3C 285.0	1.2	0.04	0.0	0.11	10778.	0.0	0.07	13471.	0.0	0.10	16168.	0.0	0.10	18860.	0.0	0.11	24249.	56.61	1,G
3C 287.0	4.7	0.40	0.90	0.03	10786.	0.92	0.03	13482.	0.92	0.04	16180.	0.94	0.08	18875.	0.93	0.03	24269.	65.28	2,Q,P
3C 286.0	10.2	0.04	CALIBRATOR																,Q,P
3C 287.1	1.8	0.04	0.25	0.03	10779.	0.42	0.03	13472.	0.07	0.03	16168.	0.24	0.03	18861.	0.22	0.03	24246.	67.76	2,G
3C 288.0	1.7	0.04	0.51	0.03	10777.	0.47	0.03	13469.	0.38	0.03	16166.	0.30	0.05	18858.	0.16	0.03	24244.	58.63	1,G
3C 289.0	1.2	0.04	0.64	0.03	10786.	0.51	0.04	13481.	0.33	0.03	16179.	0.25	0.04	18875.	0.36	0.04	24268.	53.11	1
3C 292.0	1.0	0.04	0.50	0.03	10787.	0.34	0.04	13482.	0.19	0.03	15281.							33.38	1
3C 293.0	2.9	0.04	0.74	0.03	10776.	0.73	0.03	13467.	0.72	0.04	16164.	0.71	0.04	18856.	0.64	0.03	24242.	61.91	2,G
3C 294.0	0.5	0.06	0.46	0.05	10780.	0.73	0.05	13473.	0.81	0.05	16171.	0.79	0.08	18864.	0.47	0.05	24253.	61.30	2
3C 295.0	11.7	0.10	0.95	0.03	10781.	0.98	0.03	13475.	0.95	0.03	16172.	0.94	0.04	18866.	0.92	0.05	24256.	48.73	1,G,P
3C 296.0	2.5	0.06	0.04	0.03	10776.	0.0	0.03	13468.	0.02	0.03	16165.	0.0	0.04	18856.				66.88	1
3C 298.0	2.7	0.04	0.94	0.03	10764.	0.94	0.03	13452.	0.92	0.05	16148.	0.92	0.04	18833.	0.86	0.03	24215.	67.21	2,Q,P
3C 299.0	1.6	0.04	0.88	0.03	10785.	0.93	0.03	13480.	0.97	0.03	16178.	1.04	0.03	18873.	0.90	0.04	24266.	58.59	1,G,P
3C 300.0	1.9	0.04	0.22	0.03	10750.	0.25	0.03	13445.	0.35	0.03	16135.	0.31	0.04	18824.	0.29	0.03	24195.	64.61	1,G
3C 303.0	1.5	0.04	0.0	0.03	10785.	0.0	0.03	13479.	0.0	0.03	16177.	0.0	0.04	18872.	0.0	0.03	24264.	47.90	1
3C 305.0	1.6	0.04	0.77	0.03	10787.	0.72	0.03	13482.	0.65	0.03	16179.	0.57	0.04	18876.	0.40	0.03	24269.	32.19	1,G
MSH14-1,21	2.4	0.04	0.62	0.06	10768.	0.65	0.07	13458.				0.0	0.04	18842.				68.12	2,Q
3C 309.1	5.2	0.04	0.94	0.03	10183.	0.93	0.03	12732.	0.93	0.04	15267.	0.93	0.04	17830.	0.91	0.05	22920.	77.58	1,Q,P

TABLE 2—*Continued*

SOURCE	S(2695MHZ)	P.E.	1.2KM VIS.	1.2KM P.E.	1.2KM W	1.5KM VIS.	1.5KM P.E.	1.5KM W	1.8KM VIS.	1.8KM P.E.	1.8KM W	2.1KM VIS.	2.1KM P.E.	2.1KM W	2.7KM VIS.	2.7KM P.E.	2.7KM W	P.A.	CLASS
3C 310.0	3.0	0.04	0.03	0.03	10783.	0.04	0.03	13477.	0.04	0.03	16175.	0.03	0.03	18869.	0.03	0.03	24258.	64.39	1,G
3C 313.0	1.9	0.04	0.28	0.03	10785.	0.27	0.03	13480.	0.45	0.03	16178.	0.29	0.03	18872.	0.35	0.03	24265.	67.50	1
3C 315.0	2.3	0.04	0.09	0.03	10779.	0.09	0.03	13473.	0.09	0.03	16169.	0.07	0.03	18863.	0.04	0.03	24250.	53.98	1,G
3C 317.0	2.1	0.04	0.21	0.03	10772.	0.21	0.03	13465.	0.21	0.03	16161.	0.17	0.03	18851.	0.15	0.03	24236.	57.28	1,G
3C 318.0	1.3	0.04	0.96	0.03	10786.	0.97	0.03	13481.	0.94	0.04	16179.	0.96	0.04	18874.	0.95	0.03	24267.	56.02	2,P
3C 318.1	0.0	0.01	0.0	0.50	10784.	0.0	0.50	13477.	0.0	0.50	16177.	0.0	0.50	18870.	0.0	0.50	24262.	67.46	2
3C 319.0	1.2	0.04	0.06	0.03	10787.	0.09	0.03	13482.	0.09	0.03	16180.	0.11	0.04	18876.	0.06	0.03	24269.	49.22	1
3C 320.0	0.9	0.04	0.47	0.03	10779.	0.78	0.03	13471.	0.71	0.04	16169.	0.54	0.05	18864.	0.26	0.03	24249.	60.56	2,G
3C 321.0	2.0	0.04	0.35	0.03	10758.	0.29	0.03	13444.	0.26	0.03	16133.	0.21	0.03	18826.	0.23	0.03	24197.	63.43	1
3C 322.0	0.8	0.04	0.82	0.03	10787.	0.22	0.03	13482.	0.58	0.03	16180.	0.83	0.06	18876.	0.24	0.04	24268.	47.75	1
3C 323.0	0.7	0.06	0.35	0.04	10787.	0.18	0.04	13482.	0.13	0.04	16180.	0.0	0.07	18876.	0.0	0.04	24269.	39.94	2
3C 323.1	1.3	0.04	0.26	0.03	10766.	0.49	0.03	13456.	0.48	0.03	16148.	0.20	0.03	18840.	0.33	0.03	24218.	54.65	1,Q
3C 324.0	1.3	0.04	0.39	0.03	10755.	0.55	0.03	13446.	0.77	0.03	16136.	0.84	0.06	18824.	0.86	0.03	24200.	64.19	1
3C 325.0	1.8	0.04	0.94	0.03	10786.	0.94	0.06	13482.	0.92	0.03	16180.	0.92	0.06	18875.	0.87	0.06	24270.	34.05	1,P
3C 326.1	1.3	0.10	0.67	0.03	10751.	0.66	0.03	13437.	0.54	0.03	16131.	0.52	0.04	18814.	0.65	0.03	24186.	64.40	2
3C 327.0	4.5	0.04	0.07	0.03	10777.	0.07	0.03	13468.	0.05	0.03	16167.	0.06	0.03	18858.	0.06	0.03	24246.	67.76	1,G
3C 327.1	2.1	0.04	0.19	0.03	10763.	0.07	0.03	13452.	0.27	0.03	16148.	0.43	0.03	18833.	0.45	0.03	24200.	57.73	1
3C 330.0	3.7	0.04	0.67	0.03	10253.	0.44	0.03	12794.	0.49	0.03	15356.	0.64	0.06	17913.	0.43	0.03	23056.	76.55	1
3C 332.0	1.5	0.04	0.08	0.03	10780.	0.04	0.03	13474.	0.04	0.03	16171.	0.08	0.03	18865.	0.0	0.03	24254.	52.10	1,G
3C 334.0	1.1	0.04	0.31	0.03	10782.	0.35	0.03	13475.	0.34	0.03	16173.	0.39	0.04	18866.	0.0	0.03	24257.	66.11	2,Q
MSH16-1,8	1.2	0.04	0.82	0.03	10774.	0.80	0.10	13466.	0.80	0.04	16164.	0.74	0.11	18852.	0.14	0.03	24236.	68.00	2
3C 336.0	1.4	0.04	0.78	0.03	10786.	0.68	0.03	13480.	0.28	0.03	16179.	0.39	0.03	18874.	0.61	0.03	24266.	65.25	1,Q
3C 341.0	1.1	0.04	0.22	0.03	10780.	0.17	0.03	13472.	0.13	0.03	16170.	0.0	0.03	18860.	0.14	0.03	24250.	63.51	1
3C 338.0	1.2	0.04	0.14	0.03	10786.	0.09	0.03	13482.	0.09	0.03	16180.	0.10	0.03	18876.	0.06	0.03	24269.	60.60	1,G
3C 337.0	1.5	0.05	0.47	0.03	10786.	0.65	0.03	13482.	0.51	0.03	16179.	0.57	0.03	18875.	0.32	0.03	24268.	57.59	1
3C 340.0	1.3	0.04	0.26	0.03	10784.	0.14	0.03	13479.	0.25	0.03	16177.	0.15	0.03	18872.	0.04	0.03	24261.	55.17	1
3C 343.0	2.6	0.04	0.94	0.03	10787.	0.96	0.03	13482.	0.96	0.04	16179.	0.92	0.03	18876.	0.95	0.05	24269.	34.01	1,P
3C 343.1	2.2	0.04	0.95	0.09	10787.	0.98	0.07	13482.	0.98	0.03	16180.	0.97	0.12	18876.				34.47	1,P
3C 345.0	5.9	0.06	CALIBRATOR																,Q,P
NRAO 517	1.3	0.04	1.03	0.03	10784.	1.03	0.03	13479.	1.03	0.07	16176.	1.10	0.06	18872.	1.06	0.03	24264.	66.33	1,P
3C 348.0	22.3	0.22	0.07	0.03	10783.	0.10	0.03	13478.	0.06	0.03	16176.	0.02	0.03	18871.	0.02	0.03	24263.	67.67	1,G
3C 349.0	1.9	0.04	0.69	0.03	10787.	0.59	0.03	13482.	0.50	0.03	16179.	0.37	0.03	18876.	0.36	0.03	24270.	56.07	1,G
3C 351.0	2.0	0.06	0.59	0.03	10787.	0.55	0.03	13482.	0.54	0.03	16180.	0.43	0.03	18875.	0.40	0.03	24269.	39.14	1,Q
3C 352.0	0.9	0.04	0.78	0.03	10786.	0.74	0.03	13482.	0.64	0.03	16180.	0.60	0.05	18875.	0.36	0.03	24270.	56.90	3
3C 353.0	32.3	0.50	0.02	0.03	10765.	0.01	0.03	13452.	0.01	0.03	16151.	0.01	0.03	18837.	0.01	0.03	24212.	67.91	1,G
3C 356.0	0.7	0.04	0.81	0.05	10786.	0.29	0.05	13482.	0.61	0.06	16180.	0.75	0.09	18876.	0.42	0.05	24269.	53.06	2
3C 371.0	1.9	0.10	0.71	0.03	10100.	0.73	0.03	12625.	0.69	0.05	15151.	0.64	0.06	17674.	0.61	0.05	22782.	81.42	1,G
3C 379.1	1.1	0.06	0.32	0.03	10063.	0.40	0.04	12578.	0.29	0.03	15095.				0.17	0.03	22667.	83.09	2,G
3C 380.0	9.8	0.10	0.89	0.03	10784.				0.87	0.03	15978.	0.80	0.03	18872.	0.76	0.03	24264.	54.59	2,Q
3C 390.3	6.3	0.04	0.28	0.03	10025.				0.19	0.03	15041.	0.12	0.03	17546.	0.17	0.03	22581.	85.11	1,G
3C 403.0	3.5	0.04	0.25	0.03	10787.	0.21	0.03	13482.	0.10	0.03	16180.	0.04	0.03	18876.	0.07	0.03	24269.	67.86	2
3C 410.0	5.9	0.05	0.66	0.03	10785.	0.69	0.03	13480.	0.71	0.03	16178.	0.67	0.03	18842.	0.63	0.03	24266.	63.43	3
3C 411.0	1.7	0.04	0.42	0.03	10787.	0.41	0.03	13482.	0.16	0.03	16179.	0.24	0.03	18876.	0.38	0.03	24269.	67.46	2
3C 422.0	1.4	0.04	0.95	0.03	10786.	0.88	0.03	13482.	0.89	0.04	16179.	0.91	0.04	18876.	0.90	0.04	24270.	57.89	1,P
3C 424.0	1.2	0.04	0.68	0.03	10786.	0.60	0.03	13481.	0.49	0.04	16180.	0.38	0.04	18876.	0.28	0.03	24269.	67.69	1,G
3C 432.0	0.8	0.04	0.52	0.04	10787.	0.40	0.04	13482.	0.23	0.04	16180.	0.23	0.06	18876.	0.45	0.04	24269.	66.77	2,Q
3C 433.0	6.4	0.04	0.06	0.03	10787.	0.08	0.03	13481.	0.13	0.03	16180.	0.09	0.03	18876.	0.05	0.03	24269.	65.39	2
3C 435.0	1.0	0.04	0.16	0.03	10787.	0.22	0.03	13482.	0.40	0.04	16180.	0.0	0.03	18876.	0.42	0.03	24269.	67.67	1
3C 437.0	1.5	0.05	0.91	0.03	10787.	0.89	0.03	13482.	0.82	0.06	16179.	0.71	0.03	18876.	0.62	0.03	24270.	67.00	1
NRAO 667	1.6	0.50	0.81	0.08	10786.	0.83	0.06	13482.	0.81	0.08	16180.	0.80	0.09	18876.	0.83	0.06	24270.	57.05	1,P
NRAO 668	1.3	0.04	0.76	0.03	10786.	0.66	0.03	13482.	0.74	0.04	16179.	0.76	0.04	18875.	0.86	0.03	24270.	57.08	1
3C 438.0	3.2	0.04	0.46	0.03	10786.	0.26	0.03	13482.				0.15	0.03	18876.	0.41	0.03	24269.	61.45	2
3C 441.0	1.5	0.04	0.47	0.03	10786.	0.42	0.03	13482.	0.42	0.03	16180.	0.10	0.03	18876.	0.15	0.03	24270.	64.33	1
3C 444.0	4.2	0.04	0.02	0.03	10786.	0.01	0.03	13482.	0.02	0.03	16180.	0.0	0.03	18877.	0.02	0.03	24268.	66.85	1
3C 446.0	4.2	0.05	1.00	0.03	10779.	1.04	0.03	13472.	0.95	0.06	16168.	0.92	0.04	18863.	1.00	0.03	24251.	67.99	2,Q,P
CTA 102	4.9	0.05	CALIBRATOR																,Q,P
3C 454.0	1.2	0.04	0.97	0.03	10775.	0.95	0.03	13467.	0.93	0.04	16161.	0.96	0.04	18855.	0.96	0.04	24241.	55.57	1,Q,P
3C 454.3	10.6	0.06	0.97	0.03	10786.	0.96	0.03	13482.	0.96	0.06	16179.	0.81	0.03	18876.	0.88	0.03	24269.	66.89	1,Q,P
3C 455.0	1.5	0.04	0.78	0.03	10786.	0.80	0.03	13481.	0.76	0.04	16179.	0.65	0.03	18876.	0.40	0.03	24269.	67.22	2,G
3C 456.0	1.3	0.04	0.92	0.03	10775.	0.90	0.03	13465.	0.89	0.06	16162.	0.79	0.04	18854.	0.74	0.03	24240.	67.08	1,G
3C 458.0	1.6	0.04	0.09	0.03	10787.	0.14	0.03	13482.	0.07	0.03	16179.	0.15	0.03	18876.	0.14	0.03	24270.	67.77	1,G
3C 459.0	2.2	0.04	0.69	0.03	10784.	0.58	0.03	13479.	0.55	0.03	16176.	0.62	0.03	18871.	0.72	0.03	24263.	67.72	1,G
3C 466.0	1.3	0.04	0.93	0.03	10786.	0.90	0.03	13481.	0.89	0.04	16180.	0.82	0.07	18876.	0.76	0.03	24269.	65.88	1

expected to be lower than 0.05 flux units. Thus the adopted minimum probable error in the fringe amplitude is 0.03 flux units. The effect of confusion is to increase the fractional error in the fringe visibility as one observes fainter and fainter sources. Thus, the fringe visibility of an individual source of low flux density could be in error by 15–20 per cent.

We now examine the errors introduced by calculating the fringe visibility using total flux density, and the effect of the source polarization on the measured fringe visibility. Kellermann, Pauliny-Toth, and Tyler measure the total flux density, i.e., the sum of the flux densities measured with the E-vector in position-angle 0° and 90°. The interferometer calibration scheme measures twice the flux density in position-angle 0°, except at 2.1 km where it is twice the flux density in position-angle 90°. The total flux densities for the calibration sources, given in Table 2, may be compared with those derived by the interferometer calibration scheme shown in Table 1. This comparison shows that we may expect the total flux densities to differ from those obtained by the interferometer calibration process by ± 5 per cent. Part of this difference is due to source polarization, and part is due to the fact that the flux densities of the calibration sources are on two slightly different systems. The total flux densities come from one system; the 0° position-angle fluxes in Table 1 come from a modification of that system so that the flux densities are proportional to the fringe amplitudes as seen by the interferometer.

The effect of having observed the sources at the 2.1-km separation using feeds at position-angle 90° may be seen clearly in the case of 3C 161. This source has a high percentage polarization of 9.5 per cent at a wavelength of 11 cm (Gardner and Davies 1966). Such a high polarization is apparently unusual. Of the seventy-five sources on the observing list with polarizations measured at a wavelength of 11 cm, only three have polarizations of 9.5 per cent or greater. An unresolved source, with a polarization of 10 per cent, would have a fringe visibility which differs by 20 per cent at base line 2.1 km, as compared to the other base lines in the worst case. (The worst case is the one in which the source's polarization angle is either at position-angle 0° or 90°.) In the case of a resolved source, the brightness distributions could differ in the two polarizations; hence, the effects on the fringe visibility measurement at 2.1 km are unknown, and could be larger than 20 per cent.

In some cases, equipment failure or accidental mispointing of the antennas ruined all three observations of a given source at one base line. These two causes are responsible for most of the missing information in Table 2.

Figure 2 shows the 1.2-km fringe visibility plotted against the 2.7-km fringe visibility for the sources observed. For sources having single, circular Gaussian brightness distributions, the two fringe visibilities are related as shown by the curved line. If the errors are ± 0.03 in fringe visibility, the shaded area should inclose most of the points, provided that all sources had brightness distributions of this form. In fact, this area incloses only about 25 per cent of the points. To account for the errors in the zero-spacing flux density, the shaded area should perhaps be doubled in width. If this is done, then 38 per cent of the points are inclosed. That is, 62 per cent of the sources do not have single, circular Gaussian brightness distributions. Further, sources having a single radiating component cannot have 2.7-km fringe visibilities significantly larger than the 1.2-km fringe visibilities, i.e., points in Figure 2 lying to the right of the 45° line. Errors in the zero-spacing flux density cannot cause a point to be moved across the 45° line; thus, this test is unaffected by those errors.

Table 3 displays the half-intensity width of a single Gaussian radio source which would give the various fringe visibilities at the base lines used. In Figure 2, 13 per cent of the points lie to the right of the 45° line, and these must have at least two radiating components. Allen, Brown, and Palmer (1962), using a diagram similar to Figure 2, have found that at least 60 per cent of the sources they observed are multiple.

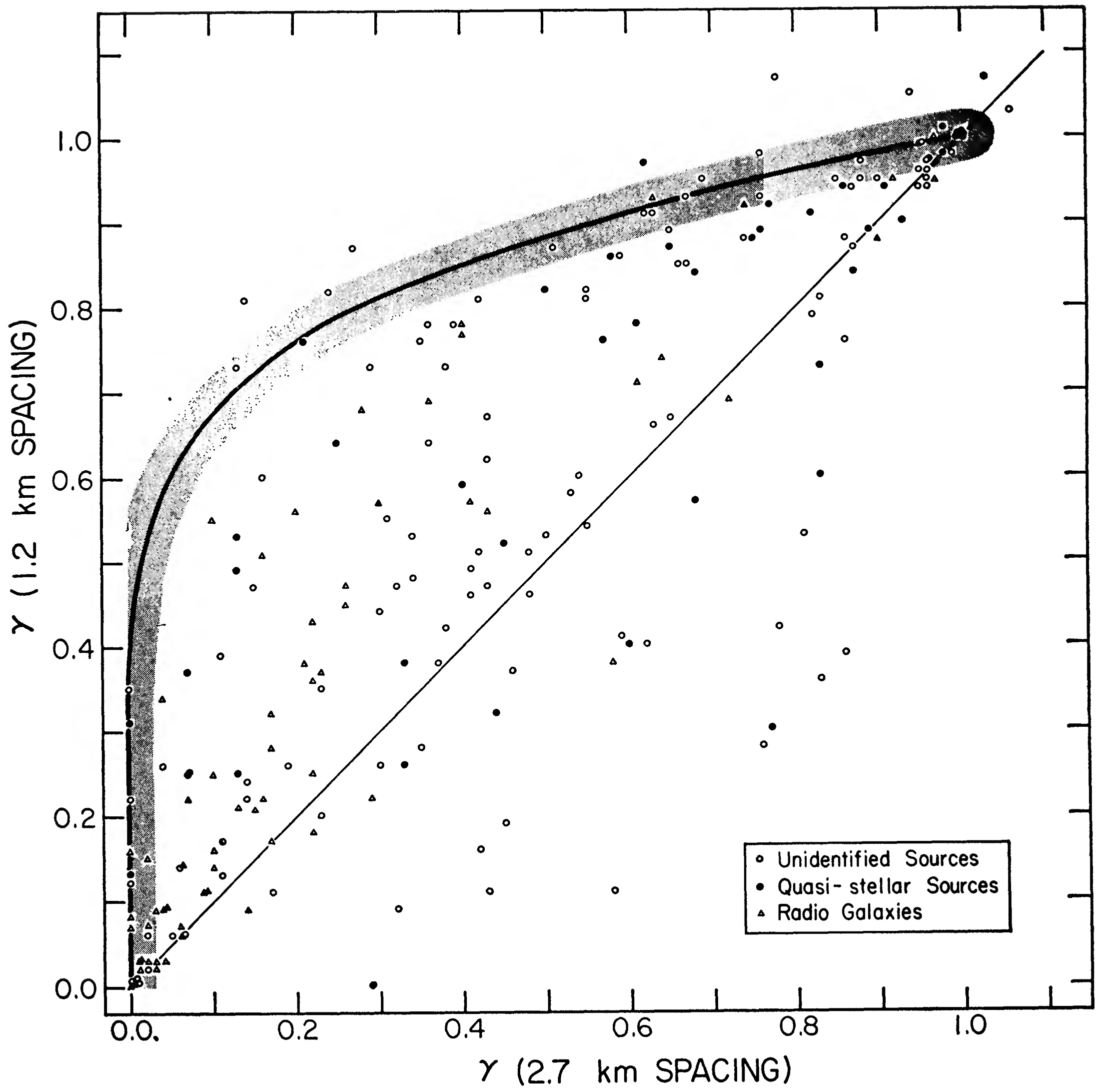

FIG. 2.—Relation between the 1.2- and the 2.7-km fringe visibilities. Radio sources with Gaussian brightness distributions should fall in the shaded area. Sources having a single component cannot lie significantly to the right of the 45° line.

TABLE 3

HALF-INTENSITY TOTAL WIDTH OF A SINGLE GAUSSIAN SOURCE GIVING THE INDICATED FRINGE VISIBILITY AT THE VARIOUS BASE LINES

FRINGE VISIBILITY	BASE LINE				
	1 2 Km	1 5 Km	1 8 Km	2 1 Km	2 7 Km
<0 1 . .	>15″4	>12″3	>10″3	>8″8	>6″8
2	12 9	10 3	8 6	7 4	5 7
4	9 7	7 8	6 5	5 5	4 3
6	7 3	5 8	4 8	4 2	3 2
8 . .	4 8	3 8	3 2	2 7	2 1
>0 9. . .	< 3 3	< 2 6	< 2 2	<1 9	<1 5

TABLE 4

NUMBER OF UNIDENTIFIED SOURCES BY VISIBILITY RANGE AT THE FIVE ANTENNA SEPARATIONS

Visibility Range	Number in Range				
	1 2 Km	1 5 Km	1.8 Km	2 1 Km	2 7 Km
0 0–0 2	21	24	27	26	24
0 2–0.4	15	25	13	18	19
0 4–0 6	21	13	21	18	23
0 6–0 8	17	23	22	24	16
0 8–1.0	36	29	32	22	22
1.0 and greater	3	5	2	3	1
Fraction with visibility >0 6	0 50	0 48	0 48	0 44	0 37

TABLE 5

NUMBER OF QUASI-STELLAR SOURCES BY VISIBILITY RANGE AT THE FIVE ANTENNA SEPARATIONS

Visibility Range	Number in Range				
	1.2 Km	1 5 Km	1 8 Km	2 1 Km	2.7 Km
0.0–0.2	2	1	4	6	6
0.2–0.4	8	8	6	8	6
0.4–0.6	5	5	6	5	5
0 6–0.8.	7	10	7	6	10
0.8–1 0	17	14	16	16	12
1.0 and greater	8	8	7	6	7
Fraction with visibility >0 6	0 65	0 70	0 65	0 60	0 63

TABLE 6

NUMBER OF RADIO GALAXIES BY VISIBILITY RANGE AT THE FIVE ANTENNA SEPARATIONS

Visibility Range	Number in Range				
	1 2 Km	1 5 Km	1 8 Km	2 1 Km	2 7 Km
0 0–0 2.	28	31	38	36	38
0 2–0 4	15	13	14	2	3
0 4–0 6	10	9	3	2	3
0 6–0 8	7	7	6	6	5
0 8–1 0	5	6	4	3	4
1 0 and greater	1	0	1	1	0
Fraction with visibility >0 6 . .	0 20	0 20	0 17	0 15	0 14

Tables 4–6 show the number of sources in intervals of 0.2 in fringe visibility at each of the five antenna separations for unidentified sources, quasi-stellar sources, and radio galaxies, respectively. In addition, the tables show the fraction of sources at each separation having visibilities greater than 0.6. The fraction with fringe visibilities greater than 0.6 is largest for the quasi-stellar sources, lower for the unidentified sources, and lowest for the radio galaxies. It is interesting to note that, for this range of spacings (greater than 2 to 1), the fraction of sources with fringe visibilities greater than 0.6 does not drop greatly at the long spacings.

We shall now examine the relation between the fringe visibilities obtained above and the following observed quantities: flux density, spectral index, redshift, and percentage polarization. As an example of the method used, we shall consider the fringe visibilities and the 2695 MHz flux density measured by Kellermann *et al.* (1967).

Table 7 shows the means of the measured fringe visibilities for the radio sources observed as a function of their 2695 MHz flux densities We have divided each identified type into two groups: those with flux densities greater than 3 flux units, and those with flux densities less than or equal to 3 flux units. We have calculated the mean of the fringe visibilities and the standard error of the mean for each group separately. We shall consider that there is a significant relation between an observed quantity (e.g., flux density) and fringe visibility when the mean visibilities of the fainter and brighter groups differ by more than twice the sum of the standard errors of the means for the two groups. Tables 8 and 9 are identical to Table 7, except that they show the relation between the fringe visibility and spectral index, and redshift.

Table 7 shows that the apparently bright quasi-stellar sources have a significantly higher mean fringe visibility than the fainter ones. Radio galaxies show a less significant relation in the opposite sense. When the quasi-stellar sources are divided at a faint flux density, say 1.5 flux units, the relation above is destroyed. The quasi-stellar sources brighter than 3 flux units show a small scatter about a high mean fringe visibility. Those fainter show a large scatter about a lower mean. The radio galaxy relation is not sensitive to the dividing flux density over the range in which enough objects lie in each group to make a reasonable test. Both the apparently brighter radio galaxies and quasi-stellar sources in this survey tend to have flatter spectra than the fainter ones. The brighter and fainter quasi-stellar sources (divided at 3 flux units) have mean $\pm$ standard error of the mean spectral indices of $\bar{\alpha} = -0.47 \pm 0.06$ and $\bar{\alpha} = -0.88 \pm 0.03$, respectively. For radio galaxies these quantities, in the same order, are: $\bar{\alpha} = -0.74 \pm 0.03$ and $\bar{\alpha} = -0.86 \pm 0.04$, respectively. This is undoubtedly enhanced as a result of observational selection. Since most of these objects were found by the 3C survey at 178 MHz, the ones with flatter radio spectra will tend to be brighter at the much higher frequency, 2695 MHz. A correlation between the physical sizes (assuming cosmological distances) and monochromatic luminosities at 3000 MHz was discovered for the quasi-stellar sources by Hogg (1966).

Table 8 shows the relation between the spectral index measured between 1400 MHz and 750 MHz and the fringe visibility. The spectral indices were taken from Pauliny-Toth *et al.* (1966). Note that we have divided the radio galaxies and unidentified sources at spectral index -0.8, while the quasi-stellar sources are divided at $\alpha = -0.65$. The median spectral index, -0.8, was initially chosen for the point of division; however, when divided at this spectral index, the quasi-stellar sources showed no significant relation between fringe visibility and spectral index. These sources show a sharp break at $\alpha = -0.65$. Those with flatter spectra have high fringe visibilities with a small scatter; those with steeper spectra (smaller α), show a larger scatter about a lower mean. No similar behavior was seen for the radio galaxies or unidentified sources; that is, moving the spectral index which divided them had no effect on the relation between spectral index and fringe visibility.

Table 8 shows that the quasi-stellar sources with $\alpha > -0.65$ have significantly higher fringe visibilities than those with $\alpha < -0.65$. No significant relation has been found between spectral index and fringe visibility for the radio galaxies or unidentified sources. The quasi-stellar sources with $\alpha > -0.65$ all have 2695 MHz flux densities greater than 4 flux units with one exception (3C 277.1). Kellermann (1964) has shown that the component separation for identified radio galaxies that are double sources tends to increase with decreasing (steepening) spectral index. Lequeux (1965) reached similar conclusions; however, he included four known quasi-stellar sources in the total list of seventy-four objects. We have found no correlation between spectral index and fringe visibility for the radio galaxies studied, over the available range of resolution. Kellermann (1966) has included quasi-stellar sources in his analysis mentioned above, and finds that for both groups the linear extent grows with decreasing spectral index.

TABLE 7

MEAN OF THE MEASURED FRINGE VISIBILITIES AS A FUNCTION OF 2695 MHz FLUX DENSITY (S)*

Quasi-stellar Sources (49)†		Radio Galaxies (68)		Unidentified (118)	
$S \leq 3$ (35)	$S > 3$ (14)	$S \leq 3$ (50)	$S > 3$ (18)	$S \leq 3$ (99)	$S > 3$ (19)
0 58±0 04. ...	0 90±0.04	0 34±0 04	0.15±0 05	0 55±0 03	0 44±0 07

* S is in flux units (10^{-26} W m^{-2} Hz^{-1}).
† The number of sources included is given in parentheses

TABLE 8

MEAN OF THE MEASURED FRINGE VISIBILITIES AS A FUNCTION OF SPECTRAL INDEX (α)*

Quasi-stellar Sources (49)†		Radio Galaxies (68)		Unidentified (110)	
$\alpha \geq -0$ 65 (11)	$\alpha < -0$ 65 (38)	$\alpha \geq -0$ 8 (33)	$\alpha < -0$ 8 (35)	$\alpha \geq -0$ 8 (42)	$\alpha < -0$ 8 (68)
0.93±0 02	0 60±0 04	0 30±0 05	0 27±0 04	0 60±0 04	0 48±0 03

* The spectral index is formed from flux-density measurements at 1400 and 750 MHz.
† The number of sources included is given in parentheses.

TABLE 9

MEAN OF THE MEASURED FRINGE VISIBILITIES AS A FUNCTION OF REDSHIFT (Z)

Quasi-stellar Sources (44)*		Radio Galaxies (36)	
$Z \leq 1$ 0 (28)	$Z > 1$ 0 (16)	$Z \leq 0$ 1 (21)	$Z > 0$ 1 (15)
0 64±0 06 ..	0 76±0.05	0 18±0 05	0 29±0 07

* The number of sources included is given in parentheses.

Table 9 shows the relation between fringe visibility and redshift (Z) for the identified quasi-stellar sources and radio galaxies. The quasi-stellar redshifts were taken from the papers cited above concerning quasi-stellar source identifications. The radio galaxy redshifts were taken from Maltby, Matthews, and Moffet (1963), Matthews, Morgan, and Schmidt (1964), Schmidt (1965), Sandage (1966), and Humason, Mayall, and Sandage (1956). No significant relation is found. However, a selection effect operates, for the quasi-stellar sources, which would confuse any real relation. Above $Z = 1.45$, the quasi-stellar sources from the 3C and 3CR catalogues all have spectral indices smaller than -0.75. This can be explained by the 3C and 3CR catalogues' selection criteria, assuming that there is a maximum integrated luminosity for quasi-stellar sources and that Hubble's law holds for quasi-stellar sources. Table 8 shows that the quasi-stellar sources with flat spectra tend to have high fringe visibilities, and these are absent from our sample at large Z.

In summary, there are significant relations between mean fringe visibility and flux density for the quasi-stellar sources and radio galaxies in opposite senses. The apparently bright quasi-stellar sources show high fringe visibilities compared to the faint ones, while the apparently bright radio galaxies show low fringe visibilities compared to the fainter ones. In addition, the quasi-stellar sources with flat radio spectra show a higher fringe visibility than those with steep radio spectra. No significant relation between spectral index and fringe visibility was found for the radio galaxies. Because of observational selection, the relation between fringe visibility and flux density for the quasi-stellar sources is affected by the relation between spectral index and fringe visibility found for them. Those objects with flat spectra and a low flux density at 2695 MHz have been discriminated against by our source selection procedure. However, there is a real absence of apparently bright quasi-stellar sources with low fringe visibility. Since no relation was discovered between spectral index and fringe visibility for the radio galaxies, we conclude that there is a real relation between flux density and fringe visibility for them. The relation is in the sense that the apparently bright radio galaxies have larger angular sizes (thus lower fringe visibilities) than the fainter ones. This relation would be expected in a simple Euclidean universe with limited ranges of their intrinsic physical sizes and radio luminosities. These relations will be discussed more fully in a subsequent paper which includes angular sizes derived from models fitted to the fringe visibilities reported in Table 2.

Finally, it is of interest to determine whether the brightness distributions of these radio sources change with frequency. The best means of presently investigating this question is a comparison of the fringe visibilities reported here, taken at 2695 MHz, with those of Allen *et al.* (1962) taken at 158 MHz. The data of Allen *et al.* include fringe visibilities measured at 9700 and 32000λ which brackets these observations in angular resolution; however, the low-frequency data have large quoted errors and are incomplete at the 32000λ spacing. Of the forty-nine quasi-stellar sources included in the present survey, thirteen have definite fringe visibilities (not upper limits) measured by Allen *et al.* at both 9700 and 32000λ. For these thirteen sources, the mean $\pm$ standard error of the mean fringe visibility at 2695 MHz is 0.85 ± 0.05. From Allen *et al.*, for the same thirteen sources, the mean of the fringe visibilities, combining both 9700 and 32000λ, is 0.73 ± 0.07. Thus, for these quasi-stellar sources, the mean fringe visibilities are not strongly different. In the case of the radio galaxies, using the same criteria as above, only nine sources are common to the two surveys. At 2695 MHz, the mean visibility is 0.67 ± 0.09, while at 158 MHz it is 0.73 ± 0.13. It is obvious that a meaningful comparison of radio-source brightness distributions at two different frequencies requires additional data.

The material in this paper formed a portion of the author's doctoral dissertation at the University of Virginia.

It is a pleasure to acknowledge many helpful discussions with Drs. S. J. Goldstein, and C. M. Wade. In addition, Drs. D. E. Hogg, B. G. Clark, and D. S. Heeschen read a preliminary draft of this paper and made many valuable comments. These observations would not have been possible without the work of Dr. W. C. Tyler and Mr. Arthur Robichaud on the receivers and equipment and the high quality of the work of the NRAO telescope operators.

REFERENCES

Allen, L. R., Anderson, B., Conway, R. G., Palmer, H. P., Reddish, V. C., and Rowson, B. 1962, *M.N.R.A.S.*, **124**, 477.
Allen, L. R., Brown, R. Hanbury, and Palmer, H. P. 1962, *M.N.R.A.S.*, **125**, 57.
Bartlett, J. F. 1966, *A.J.*, **71**, 155.
Bennett, A. S. 1962, *Mem. R.A.S.*, **68**, 163.
Burbidge, G. R., Burbidge, E. M., Hoyle, F., and Lynds, C. R. 1966, *Nature*, **210**, 774.
Clark, B. G., and Hogg, D. E. 1966, *Ap. J.*, **145**, 21.
Day, G. A., Shimmins, A. J., Ekers, R. C., and Cole, D. J. 1966, *Australian J. Phys.*, **19**, 35.
Dent, W. A. 1965, *Science*, **148**, 1458.
Fomalont, E. B. 1966, thesis, California Institute of Technology, Pasadena.
Ford, W. K., and Rubin, V. 1966, *Ap. J.*, **145**, 357.
Gardner, F. F., and Davies, R. D. 1966, *Australian J. Phys*, **19**, 441.
Hogg, D. E. 1966, *Nature*, **212**, 1336.
Humason, M. L., Mayall, N. U., and Sandage, A. R. 1956, *A.J.*, **61**, 97.
Kellermann, K. I. 1964, *Ap. J.*, **140**, 969.
———. 1966, *ibid.*, **146**, 621.
Kellermann, K. I., Pauliny-Toth, I. I. K., and Tyler, W. C. 1967 (in preparation).
Kellermann, K. I., and Read, R. B. 1965, *Pub. Owens Valley Radio Obs.*, **1**, No. 2.
Lequeux, J. 1962, *Ann. d'ap.*, **25**, 221.
———. 1965, *ibid.*, **28**, 360.
Lynds, C. R., Hill, S. J., Heere, Karen, and Stockton, A. N. 1966, *Ap. J.*, **144**, 1244.
Lynds, C. R., Stockton, A. N., and Livingston, W. C. 1965, *Ap. J.*, **142**, 1667.
Maltby, P. 1962, *Ap. J. Suppl.*, **7**, 124.
Maltby, P., Matthews, T. A., and Moffet, A. T. 1963, *Ap. J*, **137**, 153.
Matthews, T. A., Morgan, W. W., and Schmidt, M. 1964, *Ap. J.*, **140**, 35.
Mills, B. Y., Slee, O. B., and Hill, E. R., 1958, *Australian J. Phys.*, **11**, 360.
Moffet, A. T. 1962, *Ap. J. Suppl.*, **7**, 93.
Pauliny-Toth, I. I. K., Wade, C. M., and Heeschen, D. S. 1966, *Ap. J. Suppl.*, **13**, 65.
Read, R. B. 1962, *Ap. J.*, **138**, 1.
Rowson, B. 1963, *M.N.R.A.S.*, **125**, 177.
Sandage, A. 1966, *Ap. J.*, **145**, 1.
Schmidt, M. 1965, *Ap. J.*, **141**, 1.
———. 1966*a*, *ibid.*, **144**, 443.
———. 1966*b*, *I.A.U. Symp. on Instability Phenomena in Galaxies* (Bjurakan, May 1966).
Shimmins, A. J., Day, G. A., Ekers, R. D., and Cole, D. J. 1966, *Australian J. Phys.*, **19**, 837.
Wyndham, J. D. 1966, *Ap. J.*, **144**, 459.